

# Current-induced domain wall motion with adiabatic and nonadiabatic spin torques in magnetic nanowires

Z.Z. Sun<sup>1,a</sup>, J. Schliemann<sup>1</sup>, P. Yan<sup>2,b</sup>, and X.R. Wang<sup>2</sup>

<sup>1</sup> Institute for Theoretical Physics, University of Regensburg, 93040 Regensburg, Germany

<sup>2</sup> Physics Department, The Hong Kong University of Science and Technology, Clear Water Bay, Hong Kong SAR, P.R. China

Received 13 September 2010 / Received in final form 20 December 2010

Published online 1st February 2011 – © EDP Sciences, Società Italiana di Fisica, Springer-Verlag 2011

**Abstract.** We investigate current-driven domain wall (DW) propagation in magnetic nanowires in the framework of the modified Landau-Lifshitz-Gilbert equation with both adiabatic and nonadiabatic spin torque (AST and NAST) terms. By employing a simple analytical model, we can demonstrate the essential physics that any small current density can drive the DW motion along a uniaxial anisotropy nanowire even in absence of NAST, while a critical current density threshold is required due to intrinsic anisotropy pinning in a biaxial nanowire without NAST. The DW motion along the uniaxial wire corresponds to the asymptotical DW oscillation solution under high field/current in the biaxial wire case. The current-driven DW velocity weakly depends on the NAST parameter  $\beta$  in a uniaxial wire and it is similar to the  $\beta = \alpha$  case ( $\alpha$ : damping) in the biaxial wire. Apart from that, we discuss the rigid DW motion from both the energy and angular momentum viewpoints and point out some physical relations in between. We also propose an experimental scheme to measure the spin current polarization by combining both field- and current-driven DW motion in a usual flat (biaxial) nanowire.

## 1 Introduction

The domain wall (DW) motion in magnetic nanowires has recently attracted much attention in the field of nanomagnetism [1] due to the enormous potential industrial applications [2,3], such as magnetic memory bits and logic devices. Besides the field-driven DW motion [4–11], the current-induced magnetization reversal in both magnetic multilayers and nanowires through the spin torque (ST) transfer mechanism [12–14] has been massively studied, chiefly under the aspect of low power consumption and locality of electric currents. Moreover, a large number of theoretical [15–17] and experimental studies [18–22] were devoted to the current-driven DW motion. Here one distinguishes between the adiabatic spin torque (AST) which originates from the polarization of itinerant electrons adiabatically following the magnetization direction, and the nonadiabatic spin torque (NAST, often referred as a  $\beta$ -term or  $b$ -term) due to the mismatch of the current polarization and magnetic moments. For a flat magnetic nanowire exhibiting *biaxial* magnetic anisotropy, only the NAST can drive sustained DW motion at any small current density. Without NAST term, high critical current density has to be required for overcoming the intrinsic pinning from the hard-axis anisotropy, which hampers potential applications [1,15–17].

Experimental studies so far have actually been done on flat (biaxial) magnetic nanowires rather than such as cylindrical nanowires realizing the *uniaxial* anisotropy. This is mainly due to difficulties to fabricate cylindrical metallic wires by conventional lithography however there are techniques available to grow them via electrodeposition [23]. Recently no Walker breakdown was predicted for sufficiently large currents in the cylindrical wire based on a micromagnetic simulation [24]. In reference [17] it is implied that the threshold current density in a uniaxial wire vanishes due to the absence of hard-axis anisotropy based on a self-contained microscopic theory. In this paper, starting from a simple quasi-one-dimensional (1D) analytical analysis of the modified Landau-Lifshitz-Gilbert (LLG) equation, we compare the DW motion solutions in both biaxial and uniaxial nanowires. We found that, due to the small damping in usual magnetic materials, DW in a uniaxial wire moves weakly depending on the NAST parameter,  $\beta$ , and it can move even at  $\beta = 0$  (without NAST term) at any small current density. The reason is that DW motion along a uniaxial nanowire corresponds to the asymptotical solution of the DW oscillation regime under a high field/current in a biaxial nanowire case. Any small current can drive DW to move due to the absence of the intrinsic anisotropy pinning in the uniaxial wire. Furthermore, we discuss rigid DW motion from the energy and angular momentum viewpoints and point out some physical relations in between. At last, we also propose an

<sup>a</sup> e-mail: phzzsun@gmail.com

<sup>b</sup> e-mail: yanpeng@ust.hk

experimental scheme to measure the spin current polarization by combining both field and current driven DW motion in a usual flat nanowire.

## 2 Model description

A magnetic nanowire can be described as an effectively 1D continuum of magnetic moments along the wire axis direction. Magnetic domains are formed due to the competition between the anisotropic magnetic energy and the exchange interaction among adjacent magnetic moments. Without loss of generality, we shall consider a head-to-head DW structure, assuming the easy-axis being along the wire ( $z$ -) axis. Figure 1 schematically shows a magnetic nanowire and corresponding coordinate variables. A biaxial-anisotropy energy density can be formulated in terms of the magnetization vector  $\mathbf{M}$  as  $\varepsilon^K = -KM_z^2 + K_\perp M_x^2$  where  $K$  and  $K_\perp$  describe the easy- and hard-axis anisotropy, pointing along the  $z$ -axis and  $x$ -axis, respectively. The case  $K_\perp = 0$  describes a uniaxial anisotropy along the wire axis. The above energy density is given in units of  $\mu_0 M_s^2$ , where  $\mu_0$  is the vacuum permeability, and  $M_s = |\mathbf{M}|$  such that the local magnetization  $\mathbf{M}$  enters here as a unit vector,  $\mathbf{m} = \mathbf{M}/M_s$ .

If a current flows through the nanowire, the spatio-temporal magnetization dynamics is governed by the so-called modified LLG equation with additional AST and NAST terms [16,17],

$$\frac{\partial \mathbf{m}}{\partial t} = -|\gamma| \mathbf{m} \times \mathbf{H}_t + \alpha \mathbf{m} \times \frac{\partial \mathbf{m}}{\partial t} - (\mathbf{u} \cdot \nabla) \mathbf{m} + \beta \mathbf{m} \times [(\mathbf{u} \cdot \nabla) \mathbf{m}], \quad (1)$$

where  $\gamma$ ,  $\alpha$ , and  $\beta$  are the gyromagnetic ratio, the Gilbert damping coefficient, and a dimensionless coefficient describing the NAST strength, respectively.  $\beta$  is usually of the same order as the small damping in ferromagnetic metals [25–27].  $\mathbf{H}_t$  is an effective magnetic field acting on the local moments, and the velocity  $\mathbf{u}$  points along the flow direction of the itinerant electrons which is usually the wire axis although perpendicular current injection has also been investigated recently [28,29]. Thus,  $\nabla = \partial/\partial z$  in 1D, and  $u = |\mathbf{u}| = g\mu_B J P / (2eM_s)$  where  $e$ ,  $g$ ,  $\mu_B$  are the electron charge, g-factor and Bohr magneton, respectively.  $J$  and  $P$  are the density and spin polarization of the current, respectively.

The (normalized) effective field  $\mathbf{h}_t \equiv \mathbf{H}_t/M_s$  is given by the variational derivative of the total energy density (per unit section-area)  $E = \int_{-\infty}^{\infty} dz \varepsilon(z)$  with respect to magnetization,  $\mathbf{h}_t = -\delta E / \delta \mathbf{m}(z)$ . The local energy density is given by [11]

$$\varepsilon(z) = -Km_z^2 + K_\perp m_x^2 + A \left[ \left( \frac{\partial \theta}{\partial z} \right)^2 + \sin^2 \theta \left( \frac{\partial \phi}{\partial z} \right)^2 \right] - \mathbf{m} \cdot \mathbf{h}, \quad (2)$$

where  $A$  describes the exchange interaction, and  $\mathbf{h}$  is the normalized external field. Moreover, we have adopted the usual spherical coordinates (see Fig. 1),

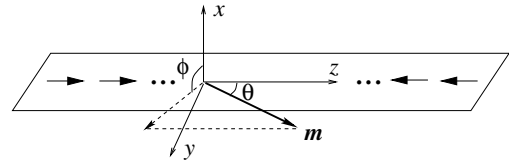


**Fig. 1.** A schematic magnetic nanowire and corresponding coordinates.

$\mathbf{m}(z, t) = (\sin \theta \cos \phi, \sin \theta \sin \phi, \cos \theta)$  where the polar angle  $\theta(z, t)$  and the azimuthal angle  $\phi(z, t)$  depend on local position and time.

Following reference [7–11], we will focus on the DW structures fulfilling  $\partial \phi / \partial z = \partial^2 \phi / \partial z^2 = 0$ , i.e. all the magnetic moments synchronously rotate around the easy-axis in space. Then the dynamical LLG equations take the form

$$\begin{aligned} \dot{\theta} + \alpha \sin \theta \dot{\phi} &= K_\perp \sin \theta \sin 2\phi + h_\phi - u \frac{\partial \theta}{\partial z}, \\ \alpha \dot{\theta} - \sin \theta \dot{\phi} &= 2A \frac{\partial^2 \theta}{\partial z^2} - K \sin 2\theta - K_\perp \sin 2\theta \cos^2 \phi \\ &\quad + h_\theta - \beta u \frac{\partial \theta}{\partial z}. \end{aligned} \quad (3)$$

Here we have introduced a dimensionless time via  $t \mapsto t|\gamma|M_s$ .  $h_i$  ( $i = r, \theta, \phi$ ) are the components of the external field in spherical coordinates.

## 3 Results

The linear DW motion under field or ST in a biaxial wire has already been discussed in the literature [7,8,16,17,30]. Let us first review the case of a flat wire with biaxial anisotropy. Following the pioneering work by Schryer and Walker [7,8] we first concentrate on solutions fulfilling  $\phi(z, t) \equiv \phi_0 = \text{const}$ . This assumption implies all the magnetic moments move in a plane which intersects the wire plane with an angle of  $(\pi/2 - \phi_0)$  (see Fig. 1) and is valid at sufficiently low field below the Walker breakdown limit [7,8]. Substituting a traveling-wave ansatz,  $\tan(\theta/2) = \exp[(z - vt)/\Delta]$ , into equations (3), we obtain

$$(1 + \alpha^2)v = \alpha \Delta h - K_\perp \Delta \sin 2\phi_0 + (1 + \alpha\beta)u, \\ \alpha K_\perp \Delta \sin 2\phi_0 + \Delta h - (\alpha - \beta)u = 0,$$

where  $\Delta \equiv \sqrt{A/(K + K_\perp \cos^2 \phi_0)}$  is the DW width depending on  $\phi_0$ , and the external field with a magnitude  $h$  along the  $z$ -axis is assumed ( $h_\theta = -h \sin \theta$ ,  $h_\phi = 0$ ). Thus, the constant plane angle  $\phi_0$  and the DW velocity satisfy

$$\sin 2\phi_0 = \frac{(\alpha - \beta)u}{\alpha K_\perp \Delta} - \frac{h}{\alpha K_\perp}, \quad v = \frac{\Delta h}{\alpha} + \frac{\beta u}{\alpha}. \quad (4)$$

This solution just recovers the Schryer-Walker result [7,8] in the presence of ST. For  $|(\alpha - \beta)u/\Delta - h| > \alpha K_\perp$  the sine in equation (4) becomes larger than unity, and the solution breaks down. Thus, the Walker breakdown field can be

formulated as  $H_w = \alpha K_\perp$  and the corresponding Walker breakdown current density  $J_w = (2eM_s/g\mu_B P)^{\frac{\alpha K_\perp \Delta}{|\alpha - \beta|}}$ . In the absence of NAST ( $\beta = 0$ ),  $J_w \propto K_\perp \Delta$ , which is in agreement with the microscopic calculation in reference [17]. In this rigid DW motion regime,  $\beta = 0$  induces zero DW velocity, i.e. NAST is necessary for sustained DW motion under any small current density in the biaxial nanowire case [16,17].

When the field and/or current is higher than the Walker breakdown limit, the DW velocity can oscillate along the biaxial nanowire. According to reference [16,30], a good approximation solution for the averaged DW velocity  $\bar{v}$  in the oscillation regime can be formulated as:

$$\bar{v} = \frac{\Delta h}{\alpha} + \frac{\beta u}{\alpha} \pm \frac{\Delta}{\alpha} \frac{\sqrt{[(\alpha - \beta)u/\Delta - h]^2 - H_w^2}}{1 + \alpha^2}, \quad (5)$$

where  $+$ / $-$  sign corresponds to the  $\alpha \geq \beta$  and  $\alpha < \beta$  case, respectively. If  $u, h \gg H_w (= \alpha K_\perp)$ , or in other way  $H_w = 0$  (i.e.  $K_\perp = 0$  for the uniaxial wire) equation (5) will explicitly reduce to the equations in the uniaxial nanowire (see Eq. (6) below). Thus, the DW motion along the uniaxial wire corresponds to the asymptotical solution of the DW oscillation regime in the biaxial case. The velocity versus current curves at different  $\beta$  can be seen in Figure 3 of reference [16].

We also note, equation (4) provides the following scheme to experimentally determine the spin polarization of the current from combining measurements of field-driven and current-driven DW motion: first perform DW velocity measurements using field and current separately, and obtain the quantities  $\Delta_{max}/\alpha \equiv C_1$  and  $\beta P/\alpha \equiv C_2$ . Here  $\Delta_{max} = \sqrt{A/K}$  is the maximum DW width and  $C_1$  can be obtained by extrapolating the data to  $h \rightarrow 0$  where  $\phi_0 = -\pi/2$ . Then apply a fixed field such that the Walker breakdown limit is reached and the DW width reaches its minimum,  $\Delta_{min} = \sqrt{A/(K + K_\perp/2)}$  where  $\phi_0 = -\pi/4$ . By injecting a spin-polarized current and subsequently changing the current density and meanwhile monitoring the increase of DW width one can reach the situation  $(\alpha - \beta)u = \Delta h$  implying  $\sin 2\phi_0 = 0$  or  $\phi_0 = -\pi/2$  and again  $\Delta = \Delta_{max}$ . (If  $\beta > \alpha$  one may reverse the current direction.) Now using  $(\alpha - \beta)P/\Delta_{max} \equiv C_3$  one can infer the current polarization  $P = C_1 C_3 + C_2$  and  $\beta/\alpha = C_2/(C_1 C_3 + C_2)$ . A large anisotropy i.e.  $K_\perp \gg K$  and the resolution for observing the DW width variation are the key points for this scheme.

Now we look at the DW motion in a uniaxial (cylindrical) wire ( $K_\perp = 0$ ). Although in reference [17] the authors have already implied that the threshold current density in a uniaxial wire vanishes in the absence of NAST, their calculations were complicated based on a self-contained microscopic model. Here we will show our simple model can also demonstrate this essential physical formulation. Using again the travelling-wave ansatz [11]:  $\tan(\theta/2) = \exp[(z - vt)/\Delta]$  where now  $\Delta = \sqrt{A/K}$ , and also for a static field  $h$  applied along the  $z$ -axis, one can straightforwardly obtain the following expressions for the velocity

and precession frequency from equation (3),

$$v = \frac{\alpha \Delta h}{1 + \alpha^2} + \frac{(1 + \alpha\beta)u}{1 + \alpha^2}, \quad \dot{\phi} = \frac{h}{1 + \alpha^2} - \frac{(\alpha - \beta)u}{(1 + \alpha^2)\Delta}. \quad (6)$$

From equation (6), due to the small damping  $\alpha$ , DW velocity weakly depends on the NAST parameter,  $\beta$ .  $v \approx u$  at  $\beta = 0$  which is similar to the  $\beta = \alpha$  case in the biaxial nanowire provided no external field is applied. As we mentioned earlier, DW motion along a uniaxial nanowire can be deduced from the oscillated DW solution under high field/current regime in the biaxial nanowire. No intrinsic pinning from the hard-axis anisotropy occurs in the uniaxial case. Hence, sustained DW motion is possible at any small current density even in the absence of NAST. In contrast, in the biaxial case, a critical current density is necessary to overcome the intrinsic pinning at  $\beta = 0$  [1,16,17]. Moreover, equation (6) also shows that, at small damping, the velocity of a current-driven DW is essentially proportional to  $u$  while in the field-driven case we have  $v \approx \alpha \Delta h$  and the DW motion is suppressed. Thus, in a uniaxial nanowire, a current is more efficient for driving a DW than an external field. Furthermore, the precessional frequency also occurs in the recently studied DW-driven electromotive force  $V_{emf} = \pm \hbar \dot{\phi}/e$  [31,32], which should also motivate future experiments in a uniaxial nanowire. The current polarization in a cylindrical wire can also be easily determined experimentally by measuring the current-driven DW velocity [24]. Besides, we would like to remark that, in general, a rigid DW solution with a form  $\theta(z, t) = f(z - vt), \phi(t) = \omega t$ , where  $f$  is a general functional expression and  $\omega$  is a constant, can not exist in the uniaxial wire with arbitrary anisotropy. Thus, a spatial dependence of  $\phi$  such as  $\phi(z, t) = \omega t + g(z - vt)$  is a more appropriate ansatz for the analytical study.

An important issue regarding technical applications of nanomagnetic phenomena is energy and its dissipation. In general, the change rate of total magnetic energy (from anisotropy, exchange interaction and external magnetic field) can be expressed as

$$\begin{aligned} \frac{dE}{dt} &= - \int_{-\infty}^{\infty} dz \frac{\partial \mathbf{m}}{\partial t} \cdot \left[ \alpha \frac{\partial \mathbf{m}}{\partial t} + u \mathbf{m} \times \frac{\partial \mathbf{m}}{\partial z} + \beta u \frac{\partial \mathbf{m}}{\partial z} \right] \\ &\equiv P_\alpha + P_{AST} + P_{NAST}. \end{aligned} \quad (7)$$

Here for the rigid DW motion,

$$\begin{aligned} P_\alpha &= -2\alpha \Delta (\dot{\phi}^2 + v^2/\Delta^2), \\ P_{AST} &= -2u\dot{\phi}, \\ P_{NAST} &= 2\beta uv/\Delta, \end{aligned} \quad (8)$$

are the total dissipation power due to the damping, the energy pumping rates done by AST and NAST, respectively. Note that the DW width  $\Delta$  follows different expressions in the biaxial and uniaxial case, and  $v$  and  $\dot{\phi}$  are given by equations (4) and (6), respectively. Remarkably, the AST does not contribute to any change in energy for a biaxial wire ( $\phi = 0$ ) below the Walker breakdown limit. Moreover, it is straightforward to verify that in both cases it

holds  $dE/dt = -2hv$  which is just the released Zeeman energy per time of a rigid DW traveling with the velocity  $v$  under the external field  $h$  [9,10]. Thus, the relation  $dE/dt = -2hv$  can also be used as a definition of the DW velocity from an energetic point of view. In particular, a moving DW driven purely by current (zero magnetic field) conserves its magnetic energy.

Let us now also discuss the dynamics of angular momentum  $\mathbf{L} = \int dz \mathbf{m}(z, t)$  (per section-area and in units of  $-\mu_0 M_s / |\gamma|$ ) due to spin-transfer mechanism. The angular momentum change due to the rigid DW motion is

$$\frac{d\mathbf{L}}{dt} = \pi\dot{\phi}\Delta\hat{e}_\phi + 2v\hat{z}, \quad (9)$$

where  $\hat{z}$  is the unit vector along the wire axis and  $\hat{e}_\phi$  is the unit vector in spherical coordinates along the latitude direction. On the other hand, the LLG equation (1) gives

$$\begin{aligned} \frac{d\mathbf{L}}{dt} &= \int_{-\infty}^{\infty} dz \left[ \mathbf{h}_t \times \frac{\partial \mathbf{m}}{\partial t} + \alpha \mathbf{m} \times \frac{\partial \mathbf{m}}{\partial t} - u \frac{\partial \mathbf{m}}{\partial z} \right. \\ &\quad \left. - \beta u \mathbf{m} \times \frac{\partial \mathbf{m}}{\partial z} \right] \\ &\equiv \boldsymbol{\Gamma}_{pre} + \boldsymbol{\Gamma}_\alpha + \boldsymbol{\Gamma}_{AST} + \boldsymbol{\Gamma}_{NAST}. \end{aligned} \quad (10)$$

For our uniaxial wire,

$$\begin{aligned} \boldsymbol{\Gamma}_{pre} &= \pi h \Delta \hat{e}_\phi, \\ \boldsymbol{\Gamma}_\alpha &= -\pi \alpha v \hat{e}_\phi + 2\alpha \dot{\phi} \Delta \hat{z}, \\ \boldsymbol{\Gamma}_{AST} &= 2u\hat{z}, \\ \boldsymbol{\Gamma}_{NAST} &= \pi \beta u \hat{e}_\phi, \end{aligned} \quad (11)$$

are the torques due to the total effective field, the damping effect, and the AST and NAST, respectively. Hence, the AST pumps longitudinal spins to the wire to push the DW propagating while the NAST and external field provide the transverse torques forcing DW precession around the wire axis. Furthermore, the damping torque  $\boldsymbol{\Gamma}_\alpha$  due to the DW precession ( $\dot{\phi}$ ) provides an extra longitudinal torque and that due to the propagation ( $v$ ) results in an effective transverse force. These two reciprocal damping effects are reminiscent of Barnett effect and Einstein-de Haas effect, respectively [33–36]. In the present case, both effects originate from nonzero damping  $\alpha \neq 0$ . Moreover, two of us have recently studied DW motion driven by a circularly polarized microwave, which also embodies the Barnett effect [37]. We also note that equation (6) can be equivalently expressed as

$$v = u + \alpha \dot{\phi} \Delta, \quad \dot{\phi} = h + \frac{\beta u}{\Delta} - \frac{\alpha v}{\Delta}, \quad (12)$$

which shows explicitly that the DW precession contributes to its velocity as  $\alpha \dot{\phi} \Delta$ , and the DW translation contributes to the precession as  $-\alpha v / \Delta$ . The above considerations refer to a uniaxial wire. In the biaxial nanowire case, however,  $\boldsymbol{\Gamma}_{pre}$  acquires an additional term from the transverse anisotropy

$$\boldsymbol{\Gamma}_{pre}^{bi} = \pi h \Delta \hat{e}_\phi - 2K_\perp \Delta \sin 2\phi \hat{z}, \quad (13)$$

and the DW precession can be absent under low field/current. As a result, the effect of AST is canceled and only NAST affects the DW velocity.

## 4 Discussion and conclusion

Before ending the paper, we would like to estimate the magnitude of DW velocity for a permalloy uniaxial or biaxial nanowire. Using permalloy parameters  $M_s = 800$  kA/m,  $\Delta = 20$  nm,  $\alpha = 0.02$ ,  $\beta = 0.04$ ,  $P = 0.4$  [4–6,16], for a uniaxial wire,  $v$  (m/s)  $\approx 0.7H$  (100 Oe)  $+ 2.9J$  ( $10^7$  A/cm $^2$ ),  $\dot{\phi}$  (GHz)  $\approx 1.76H$  (100 Oe)  $+ 0.003J$  ( $10^7$  A/cm $^2$ ) and for a flat wire,  $v$  (m/s)  $\approx 1760H$  (100 Oe)  $+ 5.8J$  ( $10^7$  A/cm $^2$ ) below the Walker limit. Thus the current-driven DW velocity has the same order in both types of wires. The field-driven azimuthal precessional frequency in a uniaxial wire is in GHz regime while current-driven precessional frequency is in MHz regime.

Among above discussions, the spin pumping effect on the DW motion can be neglected. According to reference [38], the DW-motion generated electric current density in both types of wires is less than  $\langle j_z \rangle = \frac{\hbar}{eL} (\sigma_\uparrow - \sigma_\downarrow) \frac{v}{\Delta}$ , where  $L$  is the length of the nanowire,  $\sigma_\uparrow$  and  $\sigma_\downarrow$  denote the conductivities of majority and minority electrons. In the experiments of Beach et al. [19],  $L \sim 40$   $\mu\text{m}$ ,  $\Delta \sim 20$  nm, and DW velocity  $v \sim 40\text{--}100$  m/s. For a typical conductivity  $\sigma_\uparrow \sim 10^6 \Omega^{-1} \text{ m}^{-1}$ , one can find the pumped electric current density no more than  $\langle j_z \rangle \sim 10^5\text{--}10^6 \text{ A/m}^2$ , which is much smaller than the typically applied current of the order of  $10^{10}\text{--}10^{12} \text{ A/m}^2$  in experiments [19].

In summary, we have demonstrated, in the framework of the modified LLG equation, the DW motion in a uniaxial (cylindrical) nanowire corresponds to the asymptotical oscillated solution under high field/current in a biaxial (flat) nanowire. The current-driven DW velocity in the uniaxial case weakly depends on the nonadiabatic spin torque parameter,  $\beta$ , and it is similar to the  $\beta = \alpha$  case in the biaxial nanowire. Any small current density can drive the sustained DW motion along the uniaxial wire even at  $\beta = 0$  case due to the absence of the intrinsic anisotropy pinning, which results in a critical current density threshold at  $\beta = 0$  in the biaxial nanowire. Moreover, by using the simple quasi-1D model, we have discussed the motion of a rigid DW being subject to (adiabatic or nonadiabatic) spin torques in flat or cylindrical nanowires from energetic and angular momentum viewpoints. Finally, we have also proposed an experimental scheme to measure the spin current polarization by combining both field and current driven DW motion in usual flat nanowires.

ZZS thanks the Alexander von Humboldt Foundation (Germany) for a grant. This work has been supported by Deutsche Forschungsgemeinschaft via SFB 689. PY and XRW are supported by Hong Kong RGC grants (604109 and HKU10/CRF/08-HKUST17/CRF/08).

## References

1. M. Kläui, J. Phys.: Condens. Matter **20**, 313001 (2008)
2. S.S.P. Parkin et al., Science **320**, 190 (2008)
3. D.A. Allwood et al., Science **309**, 1688 (2005)
4. T. Ono et al., Science **284**, 468 (1999)
5. D. Atkinson et al., Nature Mater. **2**, 85 (2003)
6. G.S.D. Beach et al., Nature Mater. **4**, 741 (2005)
7. N.L. Schryer, L.R. Walker, J. Appl. Phys. **45**, 5406 (1974)
8. A.P. Malozemoff, J.C. Slonczewski, *Domain Walls in Bubble Materials* (Academic, New York, 1979)
9. X.R. Wang et al., Europhys. Lett. **86**, 67001 (2009)
10. X.R. Wang et al., Ann. Phys. (N.Y.) **324**, 1815 (2009)
11. Z.Z. Sun, J. Schliemann, Phys. Rev. Lett. **104**, 037206 (2010)
12. J. Slonczewski, J. Magn. Magn. Mater. **159**, L1 (1996)
13. L. Berger, Phys. Rev. B **54**, 9353 (1996)
14. Y.B. Bazaliy et al., Phys. Rev. B **57**, R3212 (1998)
15. S. Zhang, Z. Li, Phys. Rev. Lett. **93**, 127204 (2004)
16. A. Thiaville et al., Europhys. Lett. **69**, 990 (2005)
17. G. Tatara, H. Kohno, Phys. Rev. Lett. **92**, 086601 (2004)
18. M. Kläui et al., Phys. Rev. Lett. **94**, 106601 (2005)
19. G.S.D. Beach et al., Phys. Rev. Lett. **97**, 057203 (2006)
20. M. Hayashi et al., Phys. Rev. Lett. **96**, 197207 (2006)
21. M. Hayashi et al., Phys. Rev. Lett. **98**, 037204 (2007)
22. L. Thomas et al., Nature **443**, 197 (2006)
23. A. Fert, L. Piraux, J. Magn. Magn. Mater. **200**, 338 (1999)
24. M. Yan et al., Phys. Rev. Lett. **104**, 057201 (2010)
25. S.E. Barnes, S. Maekawa, Phys. Rev. Lett. **95**, 107204 (2005)
26. Y. Tserkovnyak et al., Phys. Rev. B **74**, 144405 (2006)
27. M.D. Stiles et al., Phys. Rev. B **75**, 214423 (2007)
28. A.V. Khvalkovskiy et al., Phys. Rev. Lett. **102**, 067206 (2009)
29. C.T. Boone et al., Phys. Rev. Lett. **104**, 097203 (2010)
30. A. Thiaville, J.M. Garcia, J. Miltat, J. Magn. Magn. Mater. **242-245**, 1061 (2002)
31. S.E. Barnes, S. Maekawa, Phys. Rev. Lett. **98**, 246601 (2007)
32. S.A. Yang et al., Phys. Rev. Lett. **102**, 067201 (2009)
33. S.J. Barnett, Phys. Rev. **6**, 239 (1915)
34. S.J. Barnett, Rev. Mod. Phys. **7**, 129 (1935)
35. A. Einstein, W.J. de Haas, Deutsche Physikalische Gesellschaft, Verhandlungen **17**, 152 (1915)
36. G.E.W. Bauer et al., Phys. Rev. B **81**, 024427 (2010)
37. P. Yan, X.R. Wang, Phys. Rev. B **80**, 214426 (2009)
38. R.A. Duine, Phys. Rev. B **77**, 014409 (2008)